
Gold Exploration using Representations from a Multispectral Autoencoder

Argyro TSANTALIDOU
 Technology Innovation Institute
 Abu Dhabi, UAE
 Argyro.Tsantalidou@tii.ae

Konstantinos DOGEAS
 Technology Innovation Institute
 Abu Dhabi, UAE
 Konstantinos.Dogeas@tii.ae

Eleftheria TETOULA TSONGA
 Institute of Communication
 and Computer Systems
 Athens, Greece
 Tetoula.Tsonga@iccs.gr

Elisavet PARSELIA
 Geonova
 Athens, Greece
 Elisavet@geonova.ai

Georgios TSIMIKLIS
 Institute of Communication
 and Computer Systems
 Athens, Greece
 Georgios.Tsimiklis@iccs.gr

George ARVANITAKIS
 Technology Innovation Institute
 Abu Dhabi, UAE
 George.Arvanitakis@tii.ae

Abstract

Satellite imagery is employed for large-scale prospectivity mapping due to the high cost and (typically) limited availability of on-site mineral exploration data. In this work, we present a proof-of-concept framework that leverages generative representations learned from multispectral Sentinel-2 imagery to identify gold-bearing regions from space. An autoencoder foundation model, called Isometric, which is pretrained on the large-scale FalconSpace-S2 v1.0 dataset, produces information-dense spectral-spatial representations that serve as inputs to a lightweight XGBoost classifier. We compare this representation-based approach with a raw spectral input baseline using a dataset of 63 Sentinel-2 images from known gold and non-gold locations. The proposed method improves patch-level accuracy from 0.51 to 0.68 and image-level accuracy from 0.55 to 0.73, demonstrating that generative embeddings capture transferable mineralogical patterns even with limited labeled data. These results highlight the potential of foundation-model representations to make mineral exploration more efficient, scalable, and globally applicable.

1 Introduction

Mineral exploration is the process of identifying naturally occurring mineral deposits. As supply chains increasingly rely on these resources, efficient exploration is essential to ensure their stability Union [2024]. Assessing their economic viability for extraction and industrial use remains a crucial problem. Traditionally, mineral exploration has relied on direct field observations to infer mineral composition; and while highly accurate, these methods are time-consuming, costly, and often impractical for remote or inaccessible regions. Nevertheless, the availability of high-resolution satellite imagery from missions such as Sentinel-2 and EnMAP provides complementary data that

can reveal spectral and spatial patterns that reflect surface mineralogy that can potentially enable broader, more efficient exploration.

Machine Learning techniques are well-suited to leverage image data, as they can learn complex relationships between spectral–spatial patterns and potentially underlying mineral distributions. To this extent, several supervised models, including Support Vector Machines, Neural Networks, and Transformers, have been used to predict mineralogical composition directly from imagery Han et al. [2023]. However, these approaches require large amounts of labeled data, which are costly to obtain and often limit generalization across different sensors and regions. To address this limitation, recent studies in generative and self-supervised learning, such as Masked Autoencoders and diffusion-based models, demonstrate the ability to learn meaningful spectral–spatial structures from unlabeled data Khanna et al. [2024]. The representations produced through this process capture and organize the essential information of the input data. In satellite imagery, they capture spatial patterns and spectral behavior Hong et al. [2024].

Our contribution We create a new dataset for gold exploration. We leverage information from [Mindat.org](https://www.mindat.org) to identify locations of gold mines. Sentinel-2 images are downloaded for these locations with the addition of randomly sampled locations from the Earth.

We propose a gold exploration framework using Sentinel-2 data, where spectral–spatial representations from a generative model are fed into an XGBoost classifier. We compare the performance of this **Representations**-based method to the performance of the same XGBoost classifier that uses **Raw Input** (i.e. the 12 multispectral bands of the Sentinel-2 images). The *Representations* approach outperforms the *Raw Input* approach, improving patch-level accuracy from 0.52 to 0.68 and image-level accuracy from 0.55 to 0.73, showing the value of representation-based features for mineral exploration. We also tested the performance of the current state of the art in multispectral representation learning (SpectralGPT), and we find that the Isometric model achieves better performance.

2 Model

2.1 Generative AI Model

FalconSpace-S2v1.0 Dataset: To train our foundation model, we constructed the FalconSpace-S2v1.0 dataset comprising 1.156.800 multispectral Sentinel-2 images, each with a size of 128×128 pixels with 12 spectral bands. To ensure a comprehensive representation of Earth’s surface conditions, we implemented three sampling strategies: (1) Temporal diversity—acquisition dates selected uniformly between 01/01/2020 and 30/06/2025, capturing seasonal and environmental variations throughout the year; (2) Spatial diversity—uniform sampling across latitudes and longitudes worldwide; (3) Land cover balancing—weighted sampling according to land use/land cover (LULC) classes, giving extra weight to less representative classes and built-up areas. Finally, we ensure that all images have cloud coverage below 30%.

Autoencoder Architecture: The generative AI model used in this study follows an autoencoder architecture pretrained on the large-scale FalconSpace-S2 v1.0 dataset. Its design is based on the classical transformer-based Masked Autoencoders (MAEs, He et al. [2022]) that learn high-fidelity spectral–spatial representations from unlabeled data. The encoder is specifically adapted for multispectral imagery, following a design similar to SpectralGPT, introduced in Hong et al. [2024], where the spectral bands are grouped into $8 \times 8 \times 3$ patch tokens that preserve both spatial context and spectral continuity. In contrast to SpectralGPT, our design employs a deep decoder, with the main focus being the reconstruction quality of the full spectral cube. This gives a boost in the quality of the representations. During pretraining, random parts of the input are masked, forcing the encoder to infer missing content and capture long-range dependencies. In contrast to the commonly high masking ratio (90%) followed in the literature of vision transformers, we apply a lower masking ratio (40%) that helps the performance of the model during inference. Once trained, the encoder is **frozen** and serves as a feature extractor: its latent embeddings are later leveraged as fixed, reusable inputs in our mineral exploration pipeline to distinguish gold-bearing from non gold-bearing regions using a lightweight classifier. We apply the same strategy in both the Isometric and SpectralGPT models.

Reconstruction Performance: In order to assess the reconstruction performance of the proposed autoencoder, we use the following widely used metrics: Mean Squared Error (MSE) measures pixel-

wise differences between original and reconstructed images; Peak Signal-to-Noise Ratio (PSNR) expresses reconstruction fidelity in decibels, with higher values indicating better quality; Structural Similarity Index (SSIM) assesses perceptual similarity based on luminance, contrast, and structure; Spectral Angle Mapper (SAM) quantifies spectral distortion by measuring the angle between original and reconstructed spectra; and Relative Global Dimensional Error (ERGAS) evaluates overall radiometric consistency across all spectral bands. The following table shows the mean \pm standard deviation for each metric of our model compared to the current state of the art, i.e. SpectralGPT (Hong et al. [2024]). The arrows \downarrow and \uparrow denote *the smaller the better* and *the higher the better*, respectively.

Table 1: Reconstruction performance metrics

Method	MSE \downarrow	SAM \downarrow	ERGAS \downarrow	PSNR \uparrow	SSIM \uparrow
SpectralGPT	0.062 ± 0.037	0.217 ± 0.248	17.993 ± 49.820	21.890 ± 3.971	0.612 ± 0.0918
Isometric	0.006 ± 0.005	0.093 ± 0.261	8.359 ± 35.024	32.784 ± 3.015	0.942 ± 0.056

2.2 Mineral Exploration Model

Gold Exploration Dataset: To evaluate our representations on mineral exploration, we collected 63 Sentinel-2 images from June to August 2023: 33 images are taken from known gold deposit locations (scraped from [Mindat.org](https://www.mindat.org)) and 30 images are taken from random land locations distributed globally. Each $128 \times 128 \times 12$ image was divided into 1,024 patches of $8 \times 8 \times 3$ pixels. This process, applied to our 63 images, produced 33,792 patches from gold locations and 30,720 patches from non-gold locations. To create training and testing sets, we performed a 80/20 cross validation split at the image level, resulting in 52,224 patches (from 51 images) for training and 12,288 patches (from 12 images) for testing in each split.

We train an XGBoost patch-level classifier that assigns each patch a probability of belonging to a gold or non-gold location. During inference, we classify all 1,024 patches of an image as gold or non-gold using the XGBoost. We then aggregate these patch-level predictions through majority voting to reach a final image-level decision: gold or non-gold *location*.

This pipeline enables us to directly compare the discriminative power of learned representations versus raw multispectral input for mineral exploration.

3 Results

To evaluate the effectiveness of the learned representations compared to the raw data and the state of the art SpectralGPT, we evaluated the performance at both the patch and image levels. At the patch level (see Table 2), our representation-based approach achieved an accuracy of 0.68, compared to 0.51 for the raw baseline, achieving a considerable improvement. Our method is consistently better across the Precision, Recall, and F1-score metrics.

The patch-level Receiver Operating Characteristic-Area Under the Curve (ROC-AUC) also improved from 0.52 to 0.74, indicating better discriminative capabilities improved by 42%, as depicted in Figure 1.

At the image level (see Table 3), the accuracy increased from 0.55 to 0.73, confirming that the embeddings trained via generative reconstruction capture relevant spectral-spatial patterns associated with mineralization zones. These findings suggest that frozen generative encoders can effectively serve as universal feature extractors for resource exploration, even with limited training data. Additionally, the

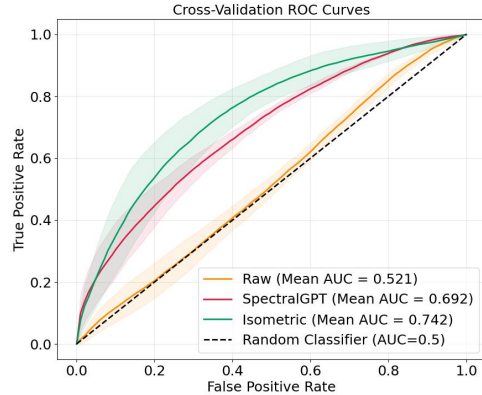


Figure 1: ROC curves illustrating the classification performance of the Raw, Spectral, and Isometric approaches.

ROC curves demonstrate that our encoder outperforms the state of the art multispectral representation model, achieving an improvement of 7.2% (see Figure 1).

Note: Given the limited amount of available data, all experiments were conducted using a 5-fold cross-validation scheme, with multiple random initializations of the train–test splits.

Table 2: Patch-level metrics (mean across folds)

Approach	Accuracy	Precision	Recall	F1 score
Raw	0.517 ± 0.010	0.513 ± 0.012	0.512 ± 0.012	0.508 ± 0.012
SpectralGPT	0.630 ± 0.011	0.642 ± 0.012	0.628 ± 0.014	0.618 ± 0.015
Isometric	0.681 ± 0.043	0.692 ± 0.042	0.680 ± 0.041	0.674 ± 0.044

Table 3: Image-level metrics (mean across folds)

Approach	Accuracy	Precision	Recall	F1 score
Raw	0.554 ± 0.101	0.551 ± 0.205	0.541 ± 0.098	0.488 ± 0.130
SpectralGPT	0.635 ± 0.039	0.683 ± 0.064	0.626 ± 0.049	0.600 ± 0.068
Isometric	0.733 ± 0.130	0.752 ± 0.141	0.733 ± 0.129	0.729 ± 0.131

In Figure 2, we show a few images from our dataset using only the visible RGB bands (3 of the 12 Sentinel-2 channels). Notably, the scenes appear practically indistinguishable to the human eye, regardless of whether they correspond to gold-bearing locations or not.



Figure 2: Gold vs Non-Gold. The three images of subfigure 2a do not contain gold, while the three images of subfigure 2b do. Using the representations of the Isometric model (our approach), XGBoost classifies correctly all six images, while using the raw input, XGBoost mislabel two out of three samples that contain gold (only the middle image of subfigure 2b is correctly predicted using raw data).

4 Conclusion

We presented a proof-of-concept study demonstrating how generative representations can enhance mineral prospectivity mapping from space. By coupling Sentinel-2 imagery with an autoencoder architecture and a lightweight XGBoost classifier, we achieved notable performance gains over raw spectral inputs. Despite using a dataset of 63 images, the results show that generative embeddings capture and can generalize across unseen regions. The frozen encoder can be reused as a fixed feature extractor for different minerals or locations, requiring only simple task-specific classifiers trained with limited labeled data. This makes satellite-based mineral prospecting more efficient, scalable, and accessible. Future work will apply this framework to larger mineral datasets, integrate SAR and hyperspectral data, and include multi-temporal analysis to better capture seasonal and surface variation in alteration zones.

References

Wei Han, Xiaohan Zhang, Yi Wang, Lizhe Wang, Xiaohui Huang, Jun Li, Sheng Wang, Weitao Chen, Xianju Li, Ruyi Feng, Runyu Fan, Xinyu Zhang, and Yuwei Wang. A survey of machine learning and deep learning in remote sensing of geological environment: Challenges, advances, and opportunities. *ISPRS Journal of Photogrammetry and Remote Sensing*, 202:87–113, 2023. doi: 10.

1016/j.isprsjprs.2023.05.032. URL <https://www.sciencedirect.com/science/article/pii/S0924271623001582>.

Kaiming He, Xinlei Chen, Saining Xie, Yanghao Li, Piotr Dollár, and Ross B. Girshick. Masked autoencoders are scalable vision learners. In *IEEE/CVF Conference on Computer Vision and Pattern Recognition, CVPR 2022, New Orleans, LA, USA, June 18-24, 2022*, pages 15979–15988. IEEE, 2022. doi: 10.1109/CVPR52688.2022.01553. URL <https://doi.org/10.1109/CVPR52688.2022.01553>.

Danfeng Hong, Bing Zhang, Xuyang Li, Yuxuan Li, Chenyu Li, Jing Yao, Naoto Yokoya, Hao Li, Pedram Ghamisi, Xiuping Jia, Antonio Plaza, Paolo Gamba, Jón Atlí Benediktsson, and Jocelyn Chanussot. Spectralgpt: Spectral remote sensing foundation model. *IEEE Trans. Pattern Anal. Mach. Intell.*, 46(8):5227–5244, 2024. doi: 10.1109/TPAMI.2024.3362475. URL <https://doi.org/10.1109/TPAMI.2024.3362475>.

Samar Khanna, Patrick Liu, Linqi Zhou, Chenlin Meng, Robin Rombach, Marshall Burke, David B. Lobell, and Stefano Ermon. Diffusionsat: A generative foundation model for satellite imagery. In *The Twelfth International Conference on Learning Representations, ICLR 2024, Vienna, Austria, May 7-11, 2024*. OpenReview.net, 2024. URL <https://openreview.net/forum?id=I5webNFDgQ>.

European Union. Regulation (eu) 2024/1252 of the european parliament and of the council of 11 april 2024 establishing a framework for ensuring a secure and sustainable supply of critical raw materials. Official Journal of the European Union L 2024/1252, 3 May 2024, 2024. URL <http://data.europa.eu/eli/reg/2024/1252/oj>.